

Particle Number Fluctuations in High Energy Nucleus-Nucleus Collisions from Microscopic Transport Approaches

V.P. Konchakovski,^{1,2} S. Haussler,³ M.I. Gorenstein,^{1,3} E.L. Bratkovskaya,³ M. Bleicher,⁴ and H. Stöcker^{3,4}

¹*Bogolyubov Institute for Theoretical Physics, Kiev, Ukraine*

²*Shevchenko National University, Kiev, Ukraine*

³*Frankfurt Institute for Advanced Studies, Frankfurt, Germany*

⁴*Institut für Theoretische Physik, Johann Wolfgang Goethe Universität, Frankfurt, Germany*

Event-by-event multiplicity fluctuations in nucleus-nucleus collisions are studied within the HSD and UrQMD transport models. The scaled variances of negative, positive, and all charged hadrons in Pb+Pb at 158 AGeV are analyzed in comparison to the data from the NA49 Collaboration. We find a dominant role of the fluctuations in the nucleon participant number for the final hadron multiplicity fluctuations. This fact can be used to check different scenarios of nucleus-nucleus collisions by measuring the final multiplicity fluctuations as a function of collision centrality. The analysis reveals surprising effects in the recent NA49 data which indicate a rather strong mixing of the projectile and target hadron production sources even in peripheral collisions.

PACS numbers: 25.75.-q, 25.75.Gz, 24.60.-k

Keywords: transport models, particle number fluctuations, mixing of hadron sources

I. INTRODUCTION

The aim of the present paper is to study particle number fluctuations in high energy nucleus-nucleus (A+A) collisions within the HSD [1] and UrQMD [2] transport approaches. The analysis of fluctuations is an important tool to study a physical system created in high energy nuclear collisions. Recently, preliminary NA49 data on particle number fluctuations in Pb+Pb collisions at 158 A GeV for different centralities have been presented [3] which are in surprising disagreement with the results of both microscopic transport models that have been shown to reproduce both the different particle multiplicities and longitudinal differential rapidity distributions for central collisions of Au+Au (or Pb+Pb) collisions from AGS to SPS energies rather well [4].

The fluctuations in high energy particle and nuclear collisions (see, e.g., Refs. [5, 6, 7, 8, 9, 10, 11, 12, 13, 14] and references therein) are studied on an event-by-event basis: a given observable is measured in each event and the fluctuations are evaluated for a specially selected set of these events. The statistical model has been successfully used to describe the data on hadron multiplicities in relativistic A+A collisions (see, e.g., Ref. [15] and a recent review [16]) as well as in elementary particle collisions [17]. This gives rise to the question whether the fluctuations, in particular the multiplicity fluctuations, do also follow the statistical hadron-resonance gas results. The statistical fluctuations can be closely related to phase transitions in QCD matter, with specific signatures for 1-st and 2-nd order phase transitions as well as for the critical point [8, 9].

In addition to the statistical fluctuations, the complicated dynamics of A+A collisions generates *dynamical* fluctuations. The fluctuations in the initial energy deposited inelastically in the statistical system yield *dynamical* fluctuations of all macroscopic parameters, like the total entropy or strangeness content. The observable consequences of the initial energy density fluctuations are sensitive to the equation of state of the matter, and can therefore be useful as signals for phase transitions [14]. Even when the data are obtained with a centrality trigger, the number of nucleons participating in inelastic collisions still fluctuates considerably. In the language of statistical mechanics, these fluctuations in participant nucleon number correspond to volume fluctuations. Secondary particle multiplicities scale linearly with the volume, hence, volume fluctuations translate directly to particle number fluctuations.

In the present paper we study the particle number fluctuations in Pb+Pb collisions at 158 AGeV within both the HSD and UrQMD transport models. We check the robustness of the two approaches and derive physical consequences from the results of the HSD and UrQMD simulations. Then we formulate a general picture of particle number fluctuations in different scenarios for A+A collision processes. The paper is organized as follows. Section II presents the HSD and UrQMD results in comparison with NA49 data. Section III studies the role of the fluctuations of the number of participant nucleons for the fluctuations of the final hadron multiplicities. HSD and UrQMD calculations are employed to clear up this point on a microscopic level. Section IV discusses a recently proposed method [18], which allows to test experimentally different model scenarios of A+A collisions. A comparison of the model results to recent NA49 data shows a necessity of strong mixing of the projectile and target hadron production sources not only for central but also for more peripheral collisions. This strong mixing is underestimated in the hadron/string dynamical approaches. Section V finally presents our summary and conclusions.

II. HSD AND URQMD RESULTS IN COMPARISON TO THE NA49 DATA

In each A+A event only a fraction of all $2A$ nucleons (the participant nucleons) interact. We denote the number of participant nucleons from the projectile and target nuclei as N_P^{proj} and N_P^{targ} , respectively. Those nucleons which do not interact are called spectator nucleons. Their numbers are related to the participant numbers as $N_S^{proj} = A - N_P^{proj}$ and $N_S^{targ} = A - N_P^{targ}$. The trivial geometrical fluctuations due to impact parameter variations usually dominate in high energy A+A collisions and mask the fluctuations of interest. One cannot fix the impact parameter experimentally, but even for a fixed impact parameter the number of participants must fluctuate from event to event. Moreover, the numbers of the projectile and the target participants differ in a given event. This is caused by fluctuations in the initial states of the colliding nuclei and the probabilistic character of the various hadron-hadron collision processes.

The NA49 Collaboration has tried to minimize the event by event fluctuations of the number of nucleon participants in measuring the multiplicity fluctuations. Samples of collisions with a fixed number of projectile spectators, $N_S^{proj} = const$, and thus a fixed number of projectile participants, $N_P^{proj} = A - N_S^{proj}$, were selected. This selection is possible in fixed target experiments, where N_S^{proj} is measured by a Zero Degree Veto Calorimeter, which covers the projectile fragmentation domain.

From an output of the HSD and UrQMD minimum bias simulations we form the samples of Pb+Pb events with fixed values of N_P^{proj} . In Fig. 1 we present the HSD and UrQMD results and compare them with the NA49 data for the scaled variances of negatively, positively, and all charged particles in Pb+Pb collisions at 158 AGeV. The average values (we will use the double brackets to denote the averaging in the model simulations),

$$\langle\langle N_i \rangle\rangle, \quad (i = +, -, ch)$$

and variances

$$Var(N_i) \equiv \langle\langle N_i^2 \rangle\rangle - \langle\langle N_i \rangle\rangle^2$$

are calculated for the samples of collision events with fixed values of the projectile participants, N_P^{proj} , and scaled variances are by definition,

$$\omega_i \equiv Var(N_i) / \langle\langle N_i \rangle\rangle.$$

Note that $\omega = 1$ for the Poisson multiplicity distribution, $P(N) = \exp(-\bar{N}) \bar{N}^N / N!$.

The final particles in the HSD and UrQMD simulations are accepted at rapidities $1.1 < y < 2.6$ (we use particle rapidities in the Pb+Pb c.m.s. frame) in accord to the NA49 transverse momentum filter [3]. This is done to compare the HSD and UrQMD results with the NA49 data. The HSD and UrQMD simulations both show flat ω_i values, $\omega_- \approx \omega_+ \approx 1.2$, $\omega_{ch} \approx 1.5$, and exhibit almost no dependence on N_P^{proj} . The NA49 data, in contrast, exhibit an enhancement in ω_i for $N_P^{proj} \approx 50$. The data show maximum values, $\omega_- \approx \omega_+ \approx 2$ and $\omega_{ch} \approx 3$, and a rather strong dependence on N_P^{proj} .

Fig. 1 also shows results of the HSD and UrQMD simulations for the full 4π acceptance for final particles, and shows the NA49-like acceptance in the mirror rapidity interval, $-2.6 < y < -1.1$ of the target hemisphere. HSD and UrQMD both result in large values of ω_i , i.e. large fluctuations in the backward hemisphere: in the backward rapidity interval $-2.6 < y < -1.1$ (target hemisphere) the fluctuations are much larger than those calculated in the forward rapidity interval $1.1 < y < 2.6$ (projectile hemisphere, where the NA49 measurements have been done). Even larger fluctuations follow from the HSD and UrQMD simulations for the full acceptance of final particles.

III. EVENT-BY-EVENT FLUCTUATIONS OF HADRON MULTIPLICITIES

The HSD and UrQMD results raise two main questions:

- What is the origin of strong fluctuations (ω_i is much larger than 1) within the HSD and UrQMD simulations both in the full acceptance and in the target hemisphere?
- Why are no large fluctuations observed in the HSD and UrQMD simulations of the NA49 acceptance, i.e. within the projectile hemisphere?

It appears that even with the rigid centrality trigger, $N_P^{proj} = const$, the number of nucleon participants still fluctuates considerably. In each sample the number of target participants fluctuates around its mean value, $\langle N_P^{targ} \rangle \approx N_P^{proj}$,

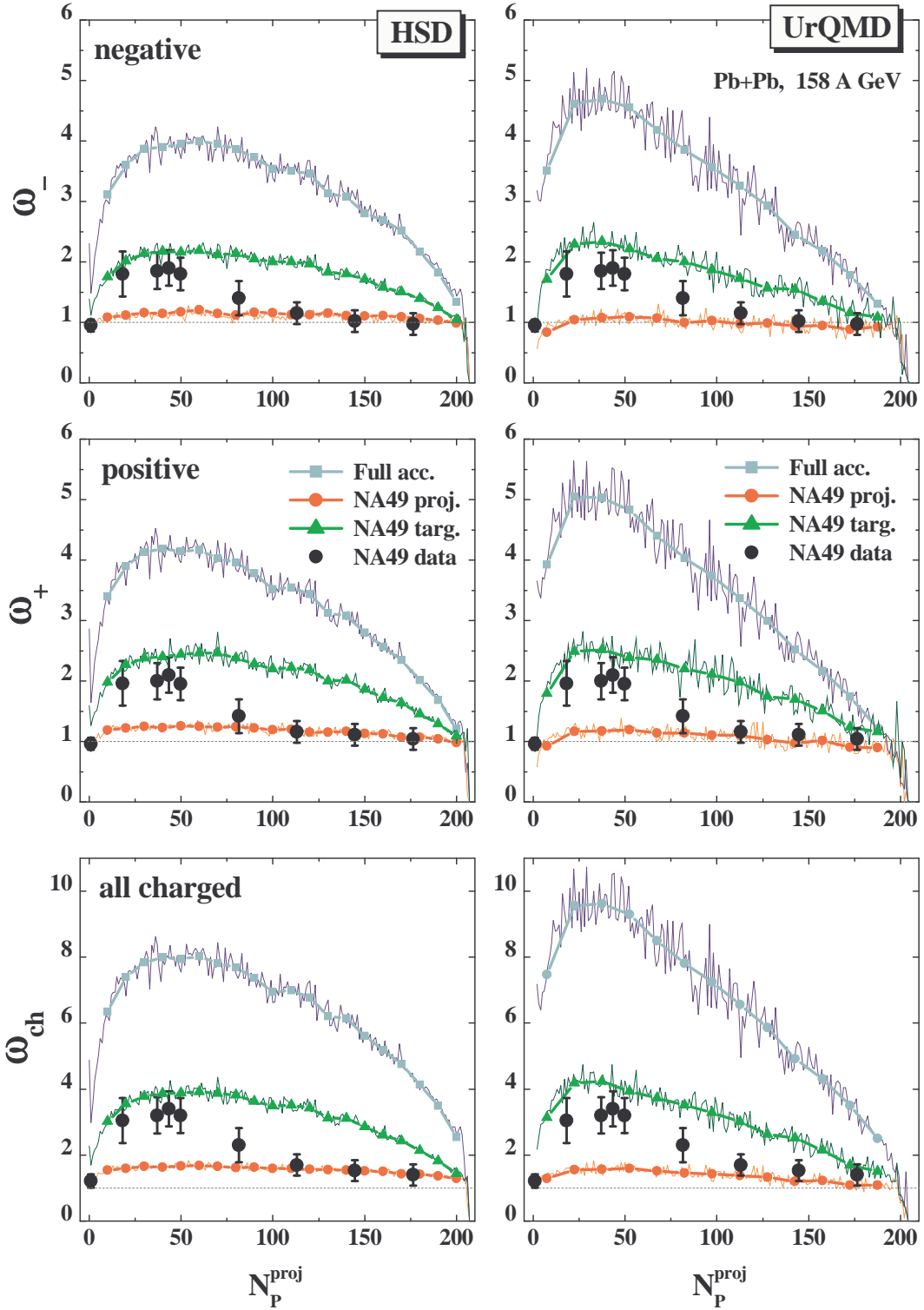


FIG. 1: The results of the HSD (left) and UrQMD (right) simulations are shown for ω_- , ω_+ , and ω_{ch} in Pb+Pb collisions at 158 AGeV as functions of N_P^{proj} . The black points are the NA49 data. The different lines correspond to the model simulations with the original NA49 acceptance, $1.1 < y < 2.6$, in the projectile hemisphere (lower lines), the NA49-like acceptance in the mirror rapidity interval, $-2.6 < y < -1.1$, in the target hemisphere (middle lines), and full 4π acceptance (upper lines).

with the variance $V(N_P^{targ}) \equiv \langle (N_P^{targ})^2 \rangle - \langle N_P^{targ} \rangle^2$. The crucial point is that by this event selection one introduces an asymmetry between projectile and target participants. The number of projectile participants is constant by con-

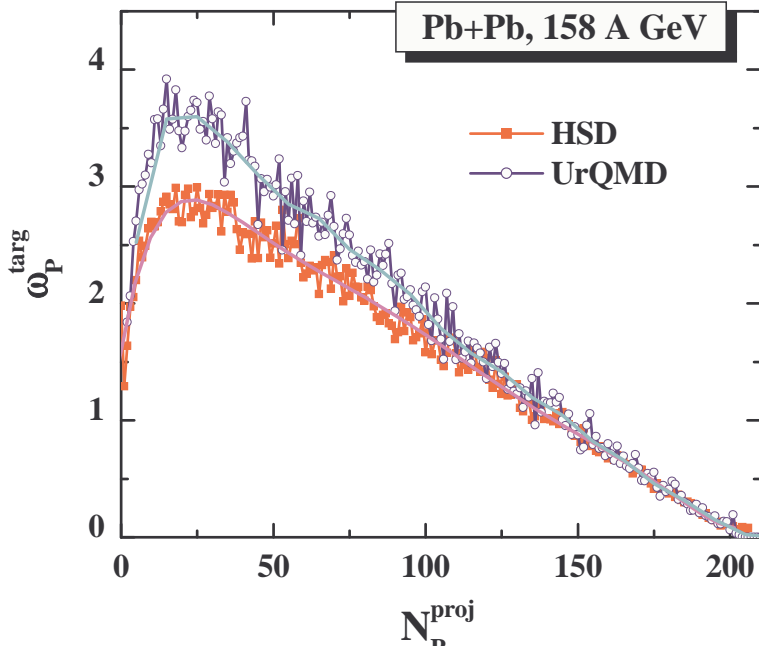


FIG. 2: HSD and UrQMD simulations show similar scaled variances ω_P^{targ} (3) as a function of N_P^{proj} .

struction, whereas the number of target participants fluctuates. What will be the consequences of this asymmetry in the final observables? As we will see later the answer depends on dynamics or properties of the model, respectively.

At fixed values of N_P^{proj} and N_P^{targ} one can introduce the average ($i = -, +, ch$; $k = 1, 2, \dots$):

$$\overline{N_i^k} \equiv \sum_{N_i \geq 0} N_i^k P(N_i | N_P^{targ}, N_P^{proj}), \quad (1)$$

where $P(N_i | N_P^{targ}, N_P^{proj})$ is the probability for producing N_i final hadrons at fixed N_P^{targ} and N_P^{proj} . In fact, only N_P^{proj} is fixed experimentally – hence, also in the HSD and UrQMD simulations presented in Fig. 1. The value of N_P^{targ} fluctuates, and we denote the average over the target participants as

$$\langle \dots \rangle \equiv \sum_{N_P^{targ} \geq 1}^A \dots W(N_P^{targ} | N_P^{proj}), \quad (2)$$

where $W(N_P^{targ} | N_P^{proj})$ is the probability for a given value of N_P^{targ} in a sample of events with fixed number of the projectile participants, N_P^{proj} . The scaled variances, ω_P^{targ} , defined as

$$\omega_P^{targ} \equiv \frac{\langle (N_P^{targ})^2 \rangle - \langle N_P^{targ} \rangle^2}{\langle N_P^{targ} \rangle}, \quad (3)$$

give a quantitative measure of the N_P^{targ} fluctuations.

Fig. 2 presents the scaled variances ω_P^{targ} calculated within the HSD and UrQMD models as functions of N_P^{proj} . The fluctuations of N_P^{targ} are quite strong; the largest value of $\omega_P^{targ} = 3 - 3.5$ occurs at $N_P^{proj} = 20 - 30$.

The total averaging procedure, $\langle \langle \dots \rangle \rangle$, performed at fixed number of projectile participants, N_P^{proj} , includes both the averaging (1) and (2), and can be therefore presented as

$$\langle \langle N_i^k \rangle \rangle \equiv \langle \overline{N_i^k} \rangle, \quad (4)$$

so that the total variance is:

$$\begin{aligned} Var(N_i) &\equiv \langle \langle N_i^2 \rangle \rangle - \langle \langle N_i \rangle \rangle^2 = \langle \overline{N_i^2} \rangle - \langle \overline{N_i} \rangle^2 \equiv \langle \overline{N_i^2} \rangle - \langle \overline{N_i} \rangle^2 + \langle \overline{N_i}^2 \rangle - \langle \overline{N_i} \rangle^2 \\ &= \langle \overline{N_i^2} - \overline{N_i}^2 \rangle + \langle \overline{N_i}^2 \rangle - \langle \overline{N_i} \rangle^2 = \omega_i^* \langle \overline{N_i} \rangle + \omega_P n_i \langle \overline{N_i} \rangle, \end{aligned} \quad (5)$$

where

$$\omega_i^* \equiv \frac{\overline{N_i^2} - \overline{N_i}^2}{\overline{N_i}} , \quad \omega_P \equiv \frac{\langle N_P^2 \rangle - \langle N_P \rangle^2}{\langle N_P \rangle} , \quad n_i \equiv \frac{\langle \overline{N_i} \rangle}{\langle N_P \rangle} , \quad (6)$$

and $N_P = N_P^{targ} + N_P^{proj}$, is the total number of participants. At the last step in Eq. (5) two assumptions have been made. First, it is assumed that ω_i^* does not depend on N_P and can be thus taken out from the averaging, $\langle \dots \rangle$, in Eq. (2). The second assumption is that the average multiplicities $\overline{N_i}$ are proportional to the number of participating nucleons, i.e. $\overline{N_i} = N_P n_i$, where n_i (defined in Eq. (6)) is the average number of particles of i -th type per participant.

Finally, the scaled variances, ω_i , can be presented as:

$$\omega_i \equiv \frac{Var(N_i)}{\langle \overline{N_i} \rangle} = \omega_i^* + \omega_P n_i . \quad (7)$$

The total number of participants fluctuates due to the fluctuations of N_P^{targ} (the values of N_P^{proj} are fixed experimentally, as well as in the HSD and UrQMD simulations). One calculates the average values, $\langle N_P^{targ} \rangle \simeq N_P^{proj}$, and scaled variances, ω_P^{targ} , for the target participants in both the HSD and UrQMD models (see Fig. 2). The scaled variance ω_P (6) for the total number of participants is easily found, $\omega_P = \omega_P^{targ}/2$, as only a half of the total number, N_P , of participants, i.e., N_P^{targ} , does fluctuate.

Putting everything together we get:

$$\omega_i = \omega_i^* + \frac{1}{2} \omega_P^{targ} n_i . \quad (8)$$

The value of ω_P^{targ} depends on N_P^{proj} , as shown by the HSD and UrQMD results in Fig. 2. The values of n_i calculated within the HSD and UrQMD simulations are presented in Fig. 3.

The Eq. (7) coincides with the result of the so called 'participant model' (see e.g., [11]), i.e. a model which treats the A+A collision as a superposition of independent nucleon-nucleon (N+N) interactions. The same result (7) can be obtained within a more general framework. One assumes that a part of the initial projectile and target energy is converted into hadron sources. The numbers of projectile and target related sources are taken to be proportional to the number of projectile and target participant nucleons, respectively. This results in Eq. (7). The physical meaning of the different sources depends on the model under consideration (e.g., wounded nucleons [19], strings and resonances [1, 2], or the fluid cells at chemical freeze-out, in the hydrodynamical models). The Eq. (7) presents the final multiplicity fluctuations as a sum of two terms: the fluctuations from one source, ω_i^* , and the contribution due to the fluctuations of the number of sources, $\omega_P n_i$.

In peripheral A+A collisions there are only few N+N collisions, and rescatterings are rare, so that the picture of independent N+N collisions looks reasonable. In this case, a hadron production source can be associated with a N+N collision and, therefore, the fluctuations from one source read:

$$\omega_i^* = \omega_i^{NN} = \frac{\alpha_{pp} \omega_i^{pp} \overline{N_i}^{pp} + \alpha_{pn} \omega_i^{pn} \overline{N_i}^{pn} + \alpha_{nn} \omega_i^{nn} \overline{N_i}^{nn}}{\alpha_{pp} \overline{N_i}^{pp} + \alpha_{pn} \overline{N_i}^{pn} + \alpha_{nn} \overline{N_i}^{nn}} , \quad (9)$$

where

$$\alpha_{pp} = Z^2/A^2 = 0.155 , \quad \alpha_{pn} = 2Z(A-Z)/A^2 = 0.478 , \quad \alpha_{nn} = (A-Z)^2/A^2 = 0.367 \quad (10)$$

are the probabilities of proton-proton, proton-neutron, and neutron-neutron collisions in Pb+Pb reactions (A=208, Z=82). The average multiplicities and scaled variances for elementary collisions calculated within the HSD simulations at 158 GeV are equal to:

$$\overline{N_{ch}}^{pp} = 6.2 , \quad \overline{N_{ch}}^{pn} = 5.8 , \quad \overline{N_{ch}}^{nn} = 5.4 , \quad (11)$$

$$\omega_{ch}^{pp} = 2.1 , \quad \omega_{ch}^{pn} = 2.4 , \quad \omega_{ch}^{nn} = 2.9 . \quad (12)$$

For negatively and positively charged hadrons, the average multiplicities and scaled variances in elementary reactions can be presented in terms of corresponding quantities for all charged particles: $\overline{N_{\pm}} = 0.5(\overline{N_{ch}} \pm \gamma)$ and $\omega_{\pm} = 0.5\omega_{ch}\overline{N_{ch}}/(\overline{N_{ch}} \mp \gamma)$, with $\gamma = 2, 1, 0$ for pp, pn and nn reactions, respectively. This yields:

$$\overline{N_{-}}^{pp} = 2.1 , \quad \overline{N_{-}}^{pn} = 2.4 , \quad \overline{N_{-}}^{nn} = 2.7 , \quad \overline{N_{+}}^{pp} = 4.1 , \quad \overline{N_{+}}^{pn} = 3.4 , \quad \overline{N_{+}}^{nn} = 2.7 , \quad (13)$$

$$\omega_{-}^{pp} = 1.55 , \quad \omega_{-}^{pn} = 1.5 , \quad \omega_{-}^{nn} = 1.45 , \quad \omega_{+}^{pp} = 0.8 , \quad \omega_{+}^{pn} = 1.0 , \quad \omega_{+}^{nn} = 1.45 . \quad (14)$$

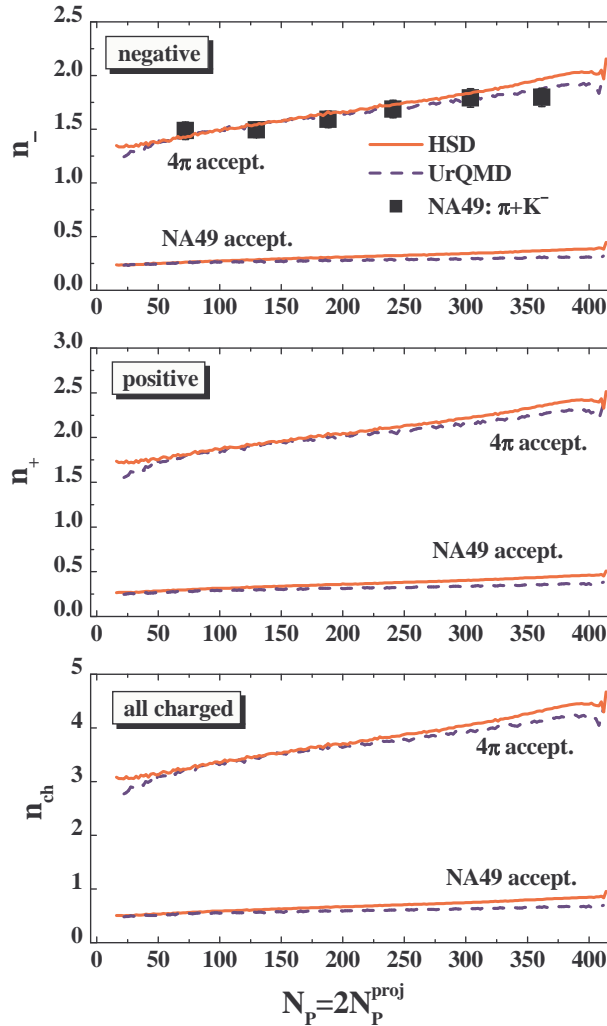


FIG. 3: The average particle number of i -th type per participant in the HSD (solid lines) and UrQMD (dashed lines) simulations for full acceptance (upper lines) and NA49 acceptance (lower lines). The symbols correspond to the experimental ratio of average $\pi + K^-$ multiplicity per nucleon [21], $\pi \equiv (\pi^- + \pi^+)/2$.

From these equations one finds the HSD results for ω_i^* per N+N collision at 158 GeV:

$$\omega_{ch}^* = 2.5, \quad \omega_-^* = 1.5, \quad \omega_+^* = 1.1. \quad (15)$$

The above arguments of the 'participant model' are not applicable for central A+A collisions, where a large degree of thermalization is expected. In the limit of $N_P^{proj} = A$ one can take the values of ω_i^* from the Pb+Pb data or model simulations. In this limit, $\omega_P = \omega_P^{targ}/2 \approx 0$ (see Fig. 2), and thus $\omega_i \approx \omega_i^*$. We have found that Eq. (15) gives a reasonable description of ω_i in the HSD simulations for central Pb+Pb collisions, too. Therefore, we will use Eqs. (8) and (15) for all values of N_P^{proj} . A comparison of Eq. (8) with the HSD simulations (accepting all final particles) is presented in Fig. 4.

The values of ω_P^{targ} and n_i are calculated within the HSD model (see Figs. 2 and 3), and for ω_i^* we use Eq. (15). As seen from Fig. 4, there is a qualitative agreement between Eq. (8) and the HSD simulations. The fluctuations of the total hadron multiplicities - generated by the HSD dynamics - are large (the ω_i are essentially larger than 1). The main contributions to ω_i come from the second terms in Eq. (8), which are due to the fluctuations of N_P^{targ} . These fluctuations of the target nucleon participants presented in Fig. 2 explain both, the large values of ω_i and their strong dependence on N_P^{proj} . Therefore, Eq. (8) takes into account two main ingredients of the multiplicity fluctuations in Pb+Pb collision: a fluctuation of the particle number created in a single N+N collision and a fluctuation in the number of nucleon participants. Fig. 4 shows that the HSD dynamics produces even larger values of ω_i than those calculated from Eq. (8). A very similar picture occurs for the UrQMD model.

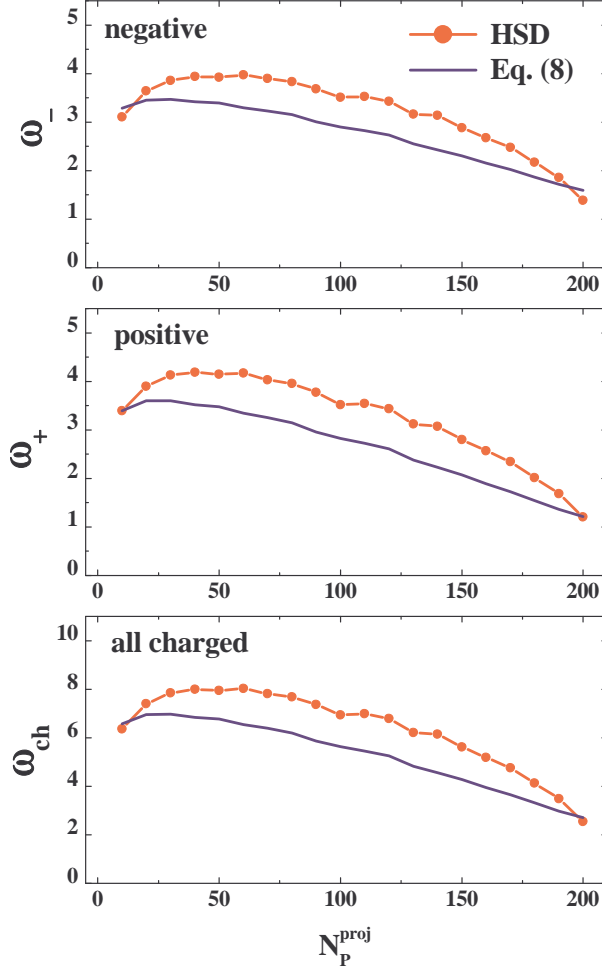


FIG. 4: The boxes are the results of the HSD simulations for ω_i in full 4π acceptance as functions of N_P^{proj} . The solid lines correspond to Eq. (8) with ω_i^* taken from Eq. (15).

Figure 5 supports the previous findings. HSD events with fixed target participant number, $N_P^{targ} = N_P^{proj}$, exhibit much smaller multiplicity fluctuations. This is due to the fact that terms proportional to ω_P^{targ} in Eq. (8) do not contribute, and ω_i become approximately equal to ω_i^* .

IV. FLUCTUATIONS IN THE PROJECTILE AND TARGET HEMISPHERES

Let us consider now the fluctuations of the particle multiplicities in the projectile ($y > 0$) and target ($y < 0$) hemispheres. As one can see from Fig. 2, in samples with $N_P^{proj} = const$ the number of target participants, N_P^{targ} , fluctuates considerably. Of course, this event selection procedure introduces an asymmetry between projectile and target participants: N_P^{proj} is constant, whereas N_P^{targ} fluctuates. Then both simulations, HSD and UrQMD, give very different results for the particle number fluctuations in the projectile and target hemispheres. The particle number fluctuations in the target hemispheres are much stronger (see Fig. 6) than those in the projectile hemispheres. There is also a strong N_P^{proj} -dependence of ω_i in the target hemisphere, which is almost absent for the ω_i in the projectile hemisphere. This is due to the asymmetry between projectile and target participants. The target participants, N_P^{targ} , play a quite small role for the particle production in the projectile hemisphere. Thus, the fluctuations of N_P^{targ} have a small influence on the final multiplicity fluctuations in the projectile hemisphere, but they contribute very strongly to those in the target hemisphere.

Different models of hadron production in relativistic A+A collisions can be divided into three limiting groups: transparency, mixing, and reflection models (see Ref. [18]). The first group assumes that the final longitudinal flows of the hadron production sources related to projectile and target participants follow in the directions of the projectile

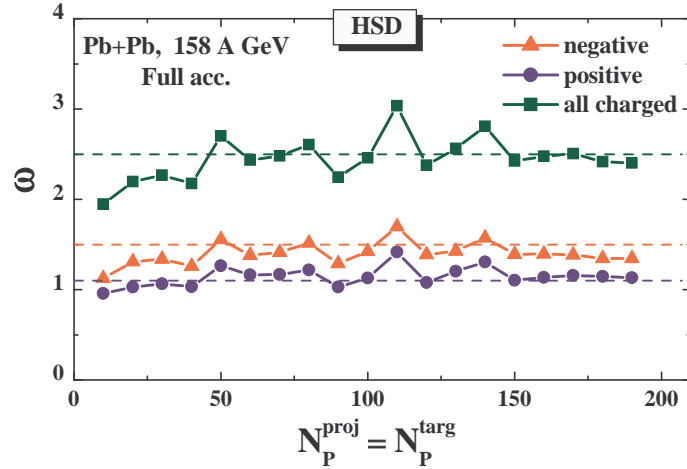


FIG. 5: The circles, triangles, and boxes are the results of the HSD simulations for ω_i in full 4π acceptance with $N_P^{targ} = N_P^{proj}$. This condition yields $\omega_P^{targ} = 0$, and Eq. (8) is reduced to $\omega_i = \omega_i^*$. The dashed lines correspond to ω_i^* taken from Eq. (15).

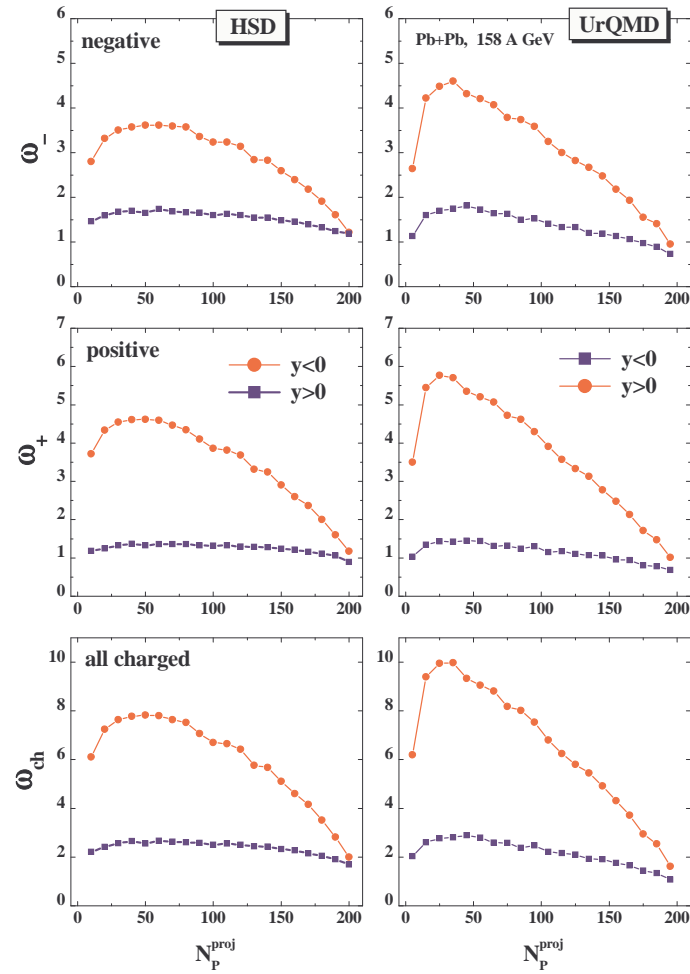


FIG. 6: The scaled variances ω_i for the projectile (boxes) and target (circles) hemispheres in the HSD (left) and UrQMD (right) simulations.

and target, respectively. We call this group of models transparency (T-)models. If the projectile and target flows of hadron production sources are mixed, we call these models the mixing (M-)models. Finally, one may even speculate

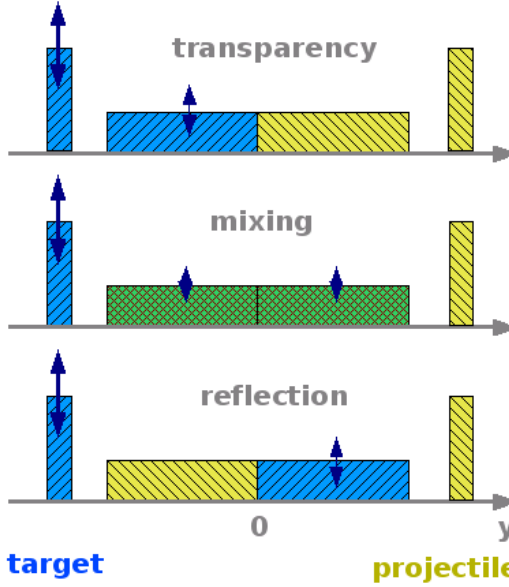


FIG. 7: The rapidity distributions of the particle production sources in nucleus-nucleus collisions resulting from transparent, mixing, and reflection models (see Ref. [18] and text for details).

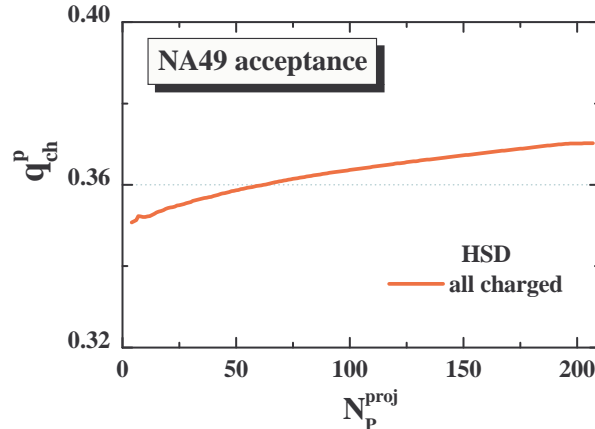


FIG. 8: The ratio of charged multiplicity within the NA49 acceptance to that in the whole projectile hemisphere. Similar results are obtained for negative and positive hadron multiplicities.

that the initial flows are reflected in the collision process. The projectile related matter then flows in the direction of the target and the target related matter flows in the direction of the projectile. This class of models we call the reflection (R-)models. The rapidity distributions resulting from the T-, M-, and R-models are sketched in Fig. 7 taken from Ref. [18].

An asymmetry between the projectile and target participants introduced by the experimental selection procedure can be used to distinguish between projectile related and target related final state flows of hadron production sources as suggested in Ref. [18]. One expects large fluctuations of hadron multiplicities in the domain of the target related flow and small fluctuations in the domain of the projectile related flow. When both flows are mixed, intermediate fluctuations are predicted. The different scenarios are presented in Fig. 7. The multiplicity fluctuations measured in the projectile momentum hemisphere clearly are larger than those measured in the target hemisphere in T-models. The opposite relation is predicted for R-models, whereas for M-models the fluctuations in the projectile and target hemispheres are expected to be the same.

In real experiments only a fraction of all final state particles is accepted. In the case of weak correlations between particles, the scaled variances in the limited acceptance can be calculated ([11, 20]) as $\omega_i^{acc} = 1 - q_i + q_i \cdot \omega_i$. Here the q_i are the probabilities that particles of type "i" are accepted. The q_i values can be calculated as the ratio of the average multiplicity of the i -th hadrons within the given experimental acceptance inside the projectile (target)

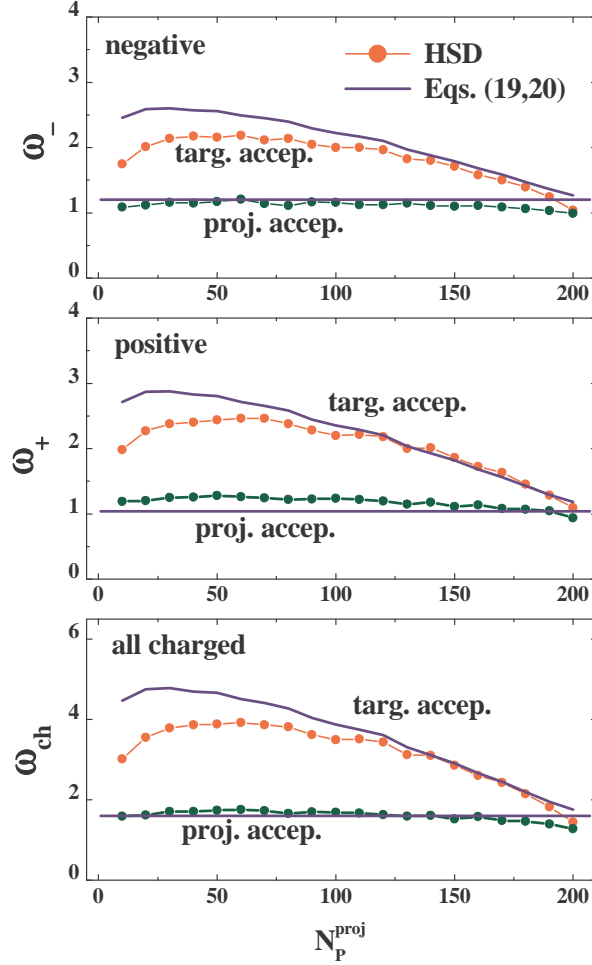


FIG. 9: The HSD simulations in the NA49 acceptance in the projectile, $1.1 < y < 2.6$, and target, $-2.6 < y < -1.1$, hemispheres. The solid lines correspond to Eqs. (19,20), which assume transparency of the longitudinal flows of the hadron production sources.

hemisphere to the average multiplicity in the whole projectile (target) hemisphere. The HSD values of $q_i^p \approx 0.36$ are presented as functions of N_P^{proj} in Fig. 8 in the NA49 acceptance (in the projectile hemisphere).

Under the above assumptions, the scaled variances of the multiplicity distributions in the projectile hemisphere, ω_i^{proj} , and target hemisphere, ω_i^{targ} , in the T-, M- and R-models read [18]:

$$\omega_i^{proj}(T) = 1 - q_i^p + q_i^p \cdot \omega_i^* , \quad \omega_i^{targ}(T) = 1 - q_i^t + q_i^t \cdot (\omega_i^* + \omega_P^{targ} n_i) , \quad (16)$$

$$\omega_i^{proj}(M) = \omega_i^{targ}(M) = 1 - q_i^{p,t} + q_i^{p,t} \cdot (\omega_i^* + 0.5 \omega_P^{targ} n_i) , \quad (17)$$

$$\omega_i^{proj}(R) = 1 - q_i^p + q_i^p \cdot (\omega_i^* + \omega_P^{targ} n_i) , \quad \omega_n^{targ}(R) = 1 - q_i^t + q_i^t \cdot \omega_i^* . \quad (18)$$

Here q_i^p and q_i^t are the acceptances in the projectile and target hemispheres, respectively.

Results presented in Fig. 6 suggest that HSD and UrQMD are closer to T-models. Using Eq. (16) the HSD simulations yield within the NA49 acceptance, and within the analogous acceptance in the mirror target rapidity interval,

$$\omega_-^{proj}(T) = 1.18 , \quad \omega_+^{proj}(T) = 1.04 , \quad \omega_{ch}^{proj}(T) = 1.54 , \quad (19)$$

$$\begin{aligned} \omega_-^{targ}(T) &= 1.18 + 0.36 \cdot \omega_P^{targ} \cdot n_- , & \omega_+^{targ}(T) &= 1.04 + 0.36 \cdot \omega_P^{targ} \cdot n_+ , \\ \omega_{ch}^{targ}(T) &= 1.54 + 0.36 \cdot \omega_P^{targ} \cdot n_{ch} . \end{aligned} \quad (20)$$

Here, the values of $q_i^p = q_i^t \approx 0.36$ are taken from the HSD calculations (Fig. 8), and the ω_i^* from Eq. (15) are used. The results of Eqs. (19,20) agree well with the HSD simulations (Fig. 9) for large projectile participant number

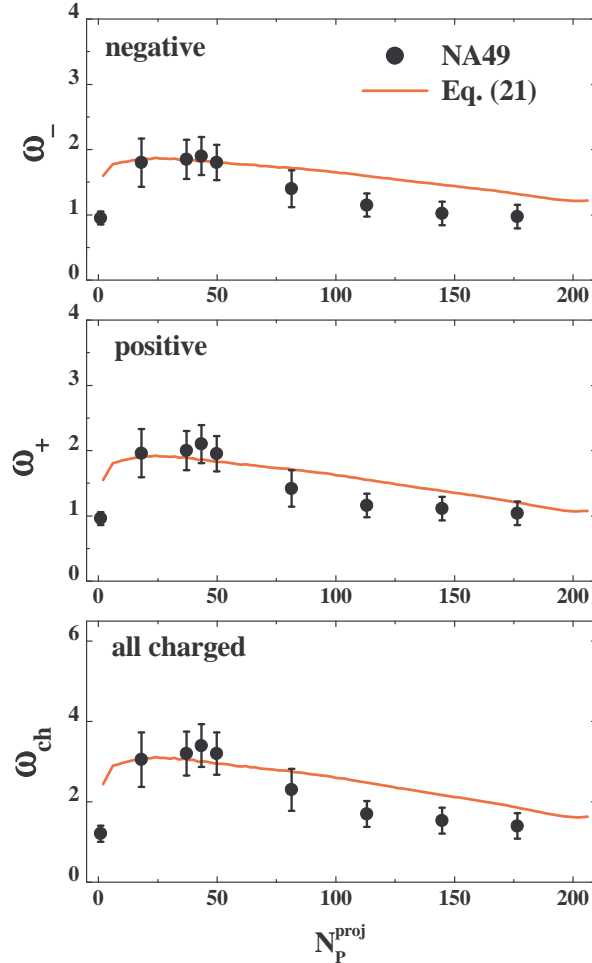


FIG. 10: The solid lines correspond to Eq. (21) with ω_i^* (15), ω_P^{targ} , and n_i taken from the HSD simulations; the points are the NA49 data.

and retain the general trend also for more peripheral collisions. Similar results are obtained within the UrQMD simulations. Hence, both the HSD and UrQMD approach are closer to T-models of hadron production sources.

Using Eq. (17) one can estimate ω_i for the NA49 acceptance in M-models. It follows:

$$\omega_i^{proj}(M) = \omega_i^{targ}(M) = 0.64 + 0.36 \cdot (\omega_i^* + 0.5 \omega_P^{targ} n_i) . \quad (21)$$

In Fig. 10 the results of Eq. (21) (with ω_i^* (15), ω_P^{targ} , and n_i taken from the HSD simulations) are compared with the NA49 data. Eq. (21) for the M-model gives a much better agreement with the NA49 data than Eq. (19) for the T-model. The NA49 data suggest therefore a large degree of mixing in the longitudinal flow of the projectile- and target hadron production sources, in agreement with suggestions formulated in Ref. [18].

Fig. 11 shows the particle number fluctuations (ω_- , ω_+ and ω_{ch}) in the HSD and UrQMD simulations, given in different rapidity intervals of the projectile ($y > 0$) and target ($y < 0$) hemispheres. The same information is presented in Fig. 12, where ω_- , ω_+ , and ω_{ch} are displayed explicitly as functions of rapidity for different N_p^{proj} values. It is clearly seen that the bias on a fixed number of projectile participants reduces strongly the particle fluctuations in the forward hemisphere, in particular within the NA49 acceptance ($1.1 < y < 2.6$). The fluctuations of the target participant numbers influence strongly the hadron production sources in the target hemispheres. They also contribute to the projectile hemisphere, but this contribution is only important in the rapidity interval $0 < y < 1$, i.e. close to midrapidity. It turns out that this "correlation length" in rapidity, $\Delta y \approx 1$, as seen in Figs. 11 and 12, is not large enough to reproduce the data. The large values of ω_i and their strong N_p^{proj} -dependence in the NA49 data (cf. Fig. 1) in the projectile rapidity interval, $1.1 < y < 2.6$, thus demonstrate a significantly larger amount of mixing in peripheral reactions than generated in simple hadron/string transport approaches.

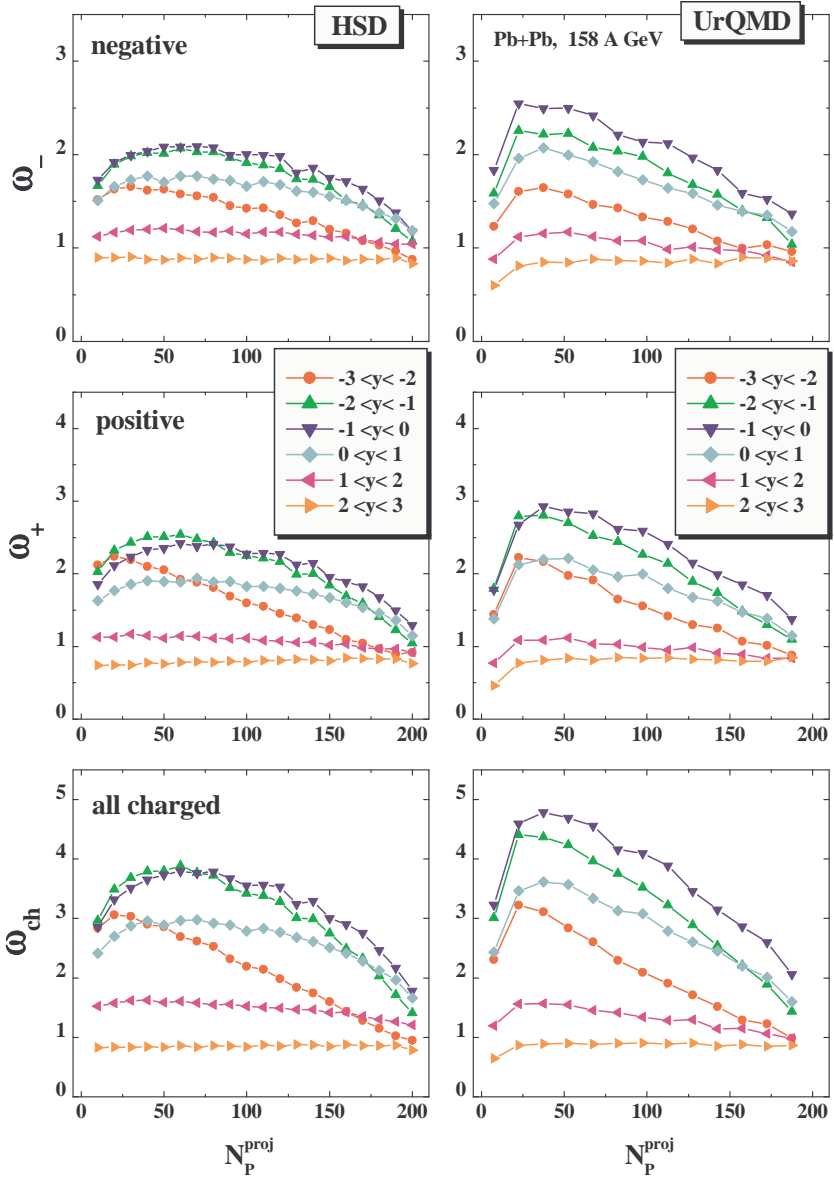


FIG. 11: Particle number fluctuations (ω_- , ω_+ , and ω_{ch}) in the HSD (left) and UrQMD simulations (right) in different rapidity intervals in the projectile ($y > 0$) and target hemispheres ($y < 0$).

V. SUMMARY AND CONCLUSIONS

The event-by-event multiplicity fluctuations in Pb+Pb collisions at 158 AGeV have been studied within the HSD and UrQMD transport models. The scaled variances of negative, positive, and all charged hadrons are analyzed in minimum bias simulations for samples of events with fixed numbers of the projectile participants, N_P^{proj} . This strong centrality trigger corresponds to the trigger of the NA49 Collaboration.

The samples with $N_P^{proj} = 20 - 60$ show the large fluctuations of the number of target nucleons, N_P^{targ} , which participate in inelastic collisions, $\omega_P^{targ} \geq 2$. The final hadron multiplicity fluctuations exhibit analogous behavior, which explains the large values of the HSD and UrQMD scaled variances ω_i in the target hemispheres and in the full 4π acceptance. On the other hand, the asymmetry between the projectile and target participants – introduced in the data samples by the trigger condition of fixed N_P^{targ} – can be used to explore different dynamics of nucleus-nucleus collisions by measuring the final multiplicity fluctuations as a function of rapidity (cf. Fig. 12). This analysis reveals that the recent NA49 data indicate a rather strong mixing of the longitudinal flows of the projectile and target hadron production sources. This is so not only for central collisions – in line with the HSD and UrQMD approaches [4] –

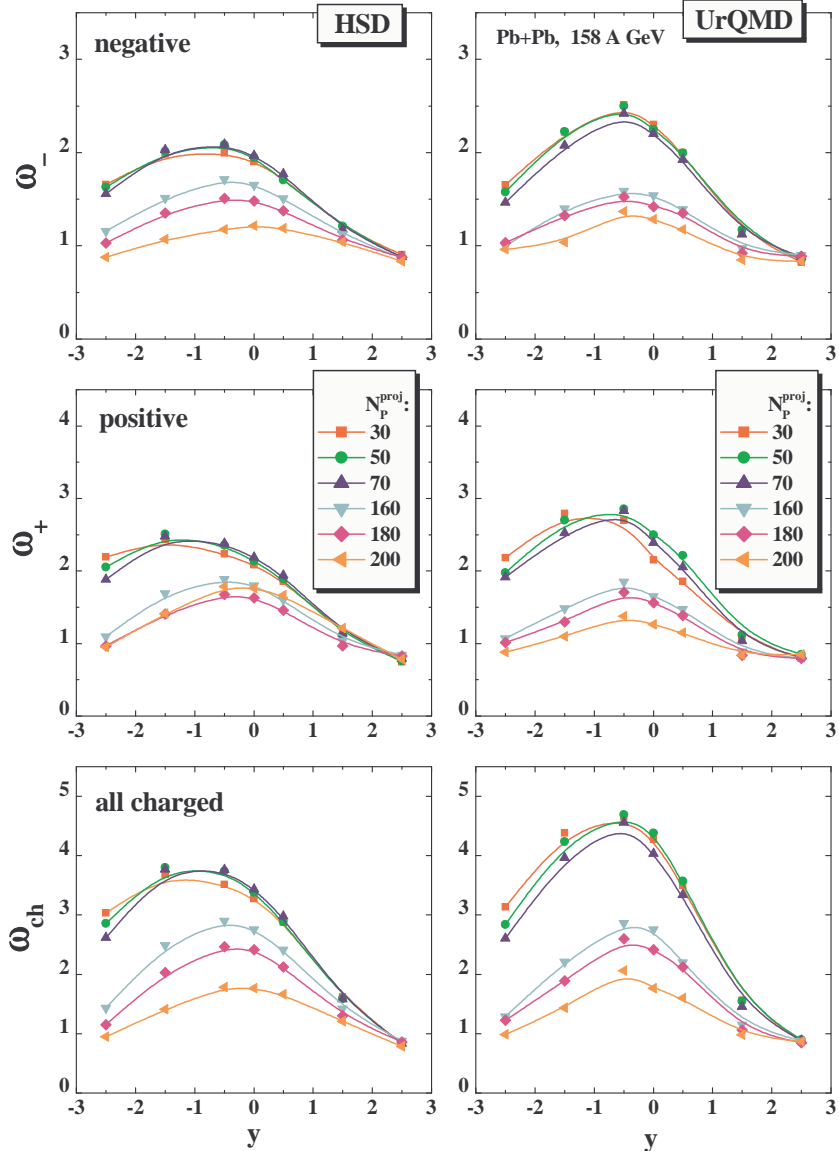


FIG. 12: Particle number fluctuations (ω_- , ω_+ , and ω_{ch}) from the HSD (left) and UrQMD (right) approaches as a function of rapidity y for different number of projectile participants N_p^{part} .

but also for rather peripheral reactions. This sheds new light on the nucleus-nucleus reaction dynamics at top SPS energies for peripheral and mid-peripheral Pb+Pb collisions. It demonstrates a significantly larger amount of mixing than is generated in simple hadron/string transport approaches.

The fluctuation analysis presented in this study can be performed in the same fashion also for higher collision energies and a related analysis in comparison to preliminary RHIC data [22] will be presented in a forthcoming study.

Acknowledgments

We would like to thank W. Cassing, M. Gazdzicki, B. Lungwitz, I.N. Mishustin, St. Mrówczyński, M. Rybczyński, and L.M. Satarov for numerous discussions. The work was supported in part by US Civilian Research and Development

[1] W. Ehehalt and W. Cassing, Nucl. Phys. A **602**, 449 (1996); W. Cassing and E.L. Bratkovskaya, Phys. Rep. **308**, 65 (1999).

[2] S.A. Bass *et al.*, Prog. Part. Nucl. Phys. **41**, 255 (1998); M. Bleicher *et al.*, J. Phys. G **25**, 1859 (1999).

[3] M. Rybczynski *et al.* [NA49 Collaboration], J. Phys. Conf. Ser. **5**, 74 (2005).

[4] H. Weber, E. L. Bratkovskaya, W. Cassing, and H. Stöcker, Phys. Rev. **C67**, 014904 (2003); E. L. Bratkovskaya, M. Bleicher, M. Reiter, S. Soff, H. Stöcker, M. van Leeuwen, S. A. Bass, and W. Cassing, Phys. Rev. **C69**, 054907 (2004); E. L. Bratkovskaya, M. Bleicher, W. Cassing, M. Reiter, S. Soff, H. Stöcker, Prog. Part. Nucl. Phys. **53**, 225 (2004).

[5] M. Gaździcki and St. Mrówczyński, Z. Phys. C **26**, 127 (1992);

[6] L. Stodolsky, Phys. Rev. Lett. **75**, 1044 (1995); E.V. Shuryak, Phys. Lett. B **423**, 9 (1998); St. Mrówczyński, Phys. Lett. B **430**, 9 (1998).

[7] G. Baym and H. Heiselberg, Phys. Lett. B **469**, 7 (1999).

[8] I.N. Mishustin, Phys. Rev. Lett. **82**, 4779 (1999); Nucl. Phys. A **681**, 56c (2001); H. Heiselberg and A.D. Jackson, Phys. Rev. C **63**, 064904 (2001).

[9] M.A. Stephanov, K. Rajagopal, and E.V. Shuryak, Phys. Rev. Lett. **81**, 4816 (1998); Phys. Rev. D **60**, 114028 (1999); M.A. Stephanov, Acta Phys. Polon. B **35**, 2939 (2004).

[10] S. Jeon and V. Koch, Phys. Rev. Lett. **83**, 5435 (1999); *ibid.* **85**, 2076 (2000).

[11] H. Heiselberg, Phys. Rep. **351**, 161 (2001).

[12] S. Jeon and V. Koch, hep-ph/0304012, Review for Quark-Gluon Plasma 3, eds. R.C. Hwa and X.-N. Wang, World Scientific, Singapore.

[13] M. Bleicher *et al.*, Nucl. Phys. A **638**, 391 (1998); Phys. Lett. B **435**, 9 (1998); Phys. Rev. C **62**, 061902 (2000); *ibid.* **62**, 041901 (2000); S. Jeon, L. Shi, and M. Bleicher, nucl-th/0506025; S. Haussler, H. Stoecker, and M. Bleicher, hep-ph/0507189.

[14] M. Gaździcki, M.I. Gorenstein, and St. Mrówczyński, Phys. Lett. B **585**, 115 (2004); M.I. Gorenstein, M. Gaździcki, and O.S. Zozulya, *ibid.* **585**, 237 (2004); M. Gaździcki, nucl-ex/0507017.

[15] H. Stöcker and W. Greiner, Phys. Rep. **137**, 277 (1986); J. Cleymans and H. Satz, Z. Phys. C **57**, 135 (1993); J. Sollfrank, M. Gaździcki, U. Heinz, and J. Rafelski, *ibid.* **61**, 659 (1994); G.D. Yen, M.I. Gorenstein, W. Greiner, and S.N. Yang, Phys. Rev. C **56**, 2210 (1997); F. Becattini, M. Gaździcki, and J. Solfrank, Eur. Phys. J. C **5**, 143 (1998); G.D. Yen and M.I. Gorenstein, Phys. Rev. C **59**, 2788 (1999); P. Braun-Munzinger, I. Heppe and J. Stachel, Phys. Lett. B **465**, 15 (1999); P. Braun-Munzinger, D. Magestro, K. Redlich, and J. Stachel, *ibid.* **518**, 41(2001); F. Becattini, M. Gaździcki, A. Keränen, J. Manninen, and R. Stock, Phys. Rev. C **69**, 024905 (2004).

[16] P. Braun-Munzinger, K. Redlich, J. Stachel, nucl-th/0304013, Review for Quark Gluon Plasma 3, eds. R.C. Hwa and X.-N. Wang, World Scientific, Singapore.

[17] F. Becattini, Z. Phys. C **69**, 485 (1996); F. Becattini, U. Heinz, *ibid.* **76**, 269 (1997); F. Becattini, G. Passaleva, Eur. Phys. J. C **23**, 551 (2002).

[18] M. Gaździcki and M.I. Gorenstein, hep-ph/0511058.

[19] A. Bialas, M. Bleszynski, and W. Czyz, Nucl. Phys. B **111**, 461 (1976).

[20] V.V. Begun, M. Gaździcki, M.I. Gorenstein, and O.S. Zozulya, Phys. Rev. C **70**, 034901 (2004).

[21] J. Bachler *et al.*, [NA49 Collaboration], Nucl. Phys. A **661**, 45 (1999).

[22] J.T. Mitchell *et al.*, [PHENIX Collaboration], nucl-ex/0511033.